MAGRITTE: an instrument suite for the Solar Atmospheric Imaging Assembly (AIA) aboard the Solar Dynamics Observatory

Pierre Rochus[a], Jean-Marc Defise[a*], Jean-Philippe Halain[a], Claude Jamar[a], Emmanuel Mazy[a], Laurence Rossi[a], Tanguy Thibert[a]
Frédéric Clette[b], Pierre Cugnon[b], David Berghmans[b], Jean-François Hochedez[b]
Jean-Pierre Delaboudinière[c], Frédéric Auchère[c]
Raymond Mercier[d], Marie-Françoise Ravet[d], Franck Delmotte[d]
Mourad Idir[e]
Udo Schühle[f], Volker Bothmer[f]
Silvano Fineschi[g]
Russel A. Howard[h] , J. Daniel Moses[h], Jeffrey Newmark[h]

[a]Centre Spatial de Liège, Av. Pré Aily, 4031 Angleur, Belgium
[b]Royal Observatory of Belgium, Av. Circulaire, Uccle, Belgium
[c]Institut d'Astrophysique Spatiale, Orsay, France
[d]Institut d'Optique Théorique et Appliquée, Orsay, France
[e]LIXAM, Orsay, France
[f]Max Planck Institut für Aeronomie, Lindau, Germany
[g]Osservatorio Astronomico di Torino, Italy
[h]Naval Research Laboratory, Washington, DC 20375

ABSTRACT

The Solar Atmospheric Imaging Assembly (AIA) aboard the Solar Dynamics Observatory will characterize the dynamical evolution of the solar plasma from the chromosphere to the corona, and will follow the connection of plasma dynamics with magnetic activity throughout the solar atmosphere. The AIA consists of 7 high-resolution imaging telescopes in the following spectral bandpasses: 1215 Å Ly-a, 304 Å He II, 629 Å OV, 465 Å Ne VII, 195 Å Fe XII (includes Fe XXIV), 284 Å Fe XV, and 335 Å Fe XVI. The telescopes are grouped by instrumental approach: the MAGRITTE Filtergraphs (R. MAGRITTE, famous 20th Century Belgian Surrealistic Artist), five multilayer EUV channels and one VUV channel, with bandpasses ranging from 195 to 1216 Å, and the SPECTRE Spectroheliograph with one soft-EUV channel at OV 629 Å. They will be simultaneously operated with a 10-second imaging cadence. These two instruments, the electronic boxes and two redundant Guide Telescopes (GT) constitute the AIA suite. They will be mounted and coaligned on a dedicated common optical bench. The GTs will provide pointing jitter information to the whole SHARPP assembly. This paper presents the selected technologies, the different challenges, the trade-offs to be made in phase A, and the model philosophy. From a scientific viewpoint, the unique combination high temporal and spatial resolutions with the simultaneous multi-channel capability will allow MAGRITTE / SPECTRE to explore new domains in the dynamics of the solar atmosphere, in particular the fast small-scale phenomena. We show how the spectral channels of the different instruments were derived to fulfill the AIA scientific objectives, and we outline how this imager array will address key science issues, like the transition region and coronal waves or flare precursors, in coordination with other SDO experiments.

Keywords: Solar Corona, EUV telescopes, spectroheliograph

[*] Correspondence:
- Email: jmdefise@ulg.ac.be, phone: +32 4 367 6668, fax: +32 4 367 5613

1. THE AIA FOR THE SDO MISSION

The Solar Dynamics Observatory (SDO) mission is part of the NASA-ILWS program; a solar observatory will be launched in 2007 and sent in a geosynchronous orbit with a quasi-permanent stable Sun pointing.

The Solar Atmospheric Imaging Assembly[1] (AIA) aboard the Solar Dynamics Observatory will be composed of two instruments: the MAGRITTE Filtergraphs, composed of six multilayer EUV / VUV channels (195 to 1216 Å), and the SPECTRE Spectroheliograph[2] (one soft-EUV channel at OV 629 Å). The AIA is part of the SHARPP program[3]. In the present paper the MAGRITTE instrument is presented.

2. THE AIA INSTRUMENT SUITE

The primary goals of the **Atmospheric Imaging Assembly** are to characterize the dynamical evolution of the solar plasma from the chromosphere to the corona, and to follow the connection of plasma dynamics with magnetic activity throughout the solar atmosphere. A global understanding of the energy balance (conductive/radiative) and energy flux can only be attained by observing emission from VUV and EUV lines that represent the full range of temperatures present in the solar atmosphere, as shown in table 1.

Chromosphere	20-80k K
Lower Transition Region (TR)	~250k K
Upper TR	~700k K
Corona	1-2 MK
hot corona	3-4 MK
Flares	e.g. 20 MK

Table 1: Typical Temperatures in the Solar corona

This investigation places particular importance in the high cadence imaging of the highly variable TR. Analysis of Differential Emission Measure (DEM) is a powerful tool to organize the study of solar atmospheric plasma with simultaneous, multi-temperature remote observations. In order to constrain the DEM model of a given line of sight in the solar atmosphere, the observations must be made in such a way as to determine the local minimums, maximums, and inflection points of the DEM curve. As can be seen from figure 1, more than five temperature regimes (five VUV & EUV lines) must be observed in order to constrain the DEM curve over the variation range of solar atmospheric plasma.

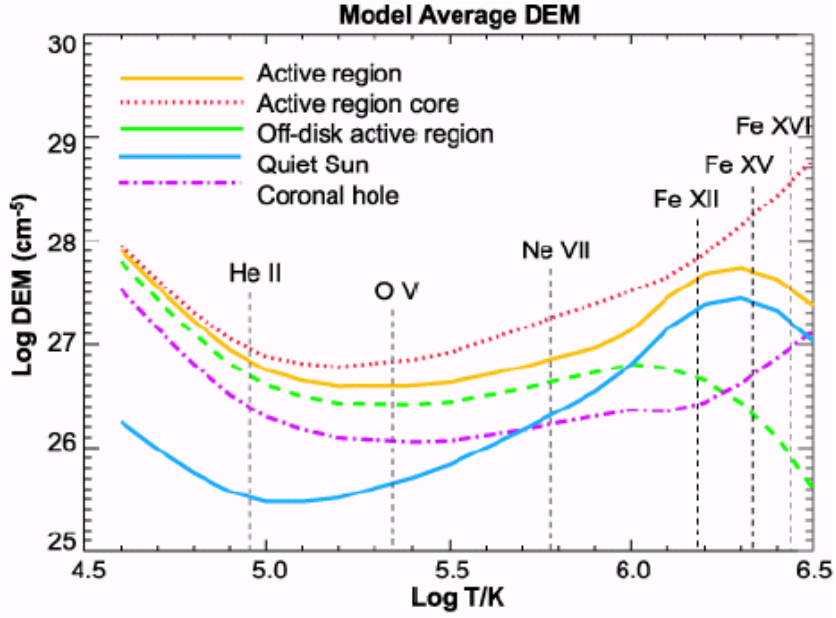

Figure 1: Differential Emission Measures, derived from EIT[4]

The selection of EUV and VUV lines for the AIA filtergraphs, from the lines observable in the solar spectrum, is further complicated by the limitations of instrumentation that can be built in a robust, low risk, resource constrained spaceflight program. The success, over the last decade, of normal incidence, multilayer-coated optics in EUV filtergraph solar telescope applications is one of the prime motivations for the SDO mission. From the EUV filtergraph technology that has been demonstrated to date and that is within the technological resources of the SHARPP consortium, we can confidently use this technique in the SDO AIA application over the wavelength regime from 500 Å to 170 Å. The short wavelength limit follows from our self-imposed restriction, on the basis of reliability over a 5-year mission, to aluminum visible light rejection filters. The extension of the long wavelength limit to a regime beyond the commonly accepted 300Å limit is achieved on the basis of recent measurements of robust Sc-W-Si-W coatings developed for an NRL laser fusion program.

Among the appropriate emission lines in the solar spectrum that are available in the 170 Å to 500 Å wavelength regime, there are three important temperature regimes that are not well characterized: the ~20,000 K chromosphere, the ~250,000 K lower transition region, and the 5-10 MK active region core.

a. The low chromosphere will be observed in AIA with a vacuum ultraviolet (VUV) filtergraph tuned to 1215Å Ly-α emission line. The techniques demonstrated in the CNES Transition Region Camera[5] (TRC) program two decades ago provide a robust system for this filtergraph.
b. The ~250,000K lower transition region poses a larger problem in that there are no lines in even the VUV that are available to use in a robust filtergraph. Thus, we must resort to spectroheliographic techniques. The 629Å OV line was chosen for its relative intensity and isolation from adjacent lines. The ~0.1Å broadening typical of lines in the turbulent transition region requires a low dispersion system to prevent the line width from destroying the high spatial resolution in the direction of dispersion. However, the proximity of the 609Å MgX line and the need for a FOV of a solar diameter, requires a high dispersion system. These dual requirements eliminate the use of a simple Cassegrain-Wadsworth design (e.g. in 9) and require a more complex system derived from the zero net dispersion system of Prinz[8]. Current technology, as demonstrated by one of our potential gratings source (Jobin-Yvon), in an extremely conservative proof-of-principle design, described below, can provide OV observations with the cadence required for the SDO science.
c. We have chosen to follow the specific temperature range described in the SDO AO (20,000 K to 4 MK) and not observe the temperature characteristic of the high temperature peak of active region cores, relying instead on the limits placed by observations of Fe XVI and Fe XXIV. The restriction to aluminum visible-light rejection filters prevents the observation of EUV line candidates for this temperature regime. The envelope restriction of the SDO mission prevents the use of a grazing incidence system for observing AR core plasma.

The SHARPP/AIA consists of 7 telescopes imaging the following bandpasses: 1215 Å Ly-α, 304 Å He II, 629 Å OV, 465 Å Ne VII, 195 Å Fe XII (includes Fe XXIV), 284 Å Fe XV, and 335 Å Fe XVI.

The telescopes are grouped by instrumental approach:

(1) **MAGRITTE Filtergraphs**: five multilayer "EUV channels", with bandpasses ranging from 195 to 500 Å and one Ly-α channel;
(2) **SPECTRE Spectroheliograph[2]**: one "soft EUV channel" O_V at 630 Å.

These two instruments, the electronic boxes and two Guide Telescopes (GT) constitute the AIA suite. They will be mounted and coaligned on two dedicated common optical benches. The GTs will provide pointing jitter information to the whole SHARPP suite through an Image Motion Compensation System. The CCD cameras for the AIA are common to the seven telescopes. The seven AIA cameras will image the Sun simultaneously at a 10 second cadence with a 0.66"/pixel resolution in a field of view extending from the Sun center to 1.4 $R_\odot$. The extended FOV is required to have sufficient overlap with the complementary EUV coronagraphs observations.

Table 2: AIA Characteristics	
Instrument Type	- 6 Filtergraphs (MAGRITTE) - Spectroheliograph (SPECTRE) - 2 Guide Telescopes for IMC (Image Motion Compensation System)
Observable	Emission Line Chromosphere, Transition Region & Corona
Data Products	Images, Maps of Temperature & DEM
FOV (Rs)	• Full disk to 1.4 (MAGRITTE) • Full disk to 1.3 (SPECTRE)
Spatial Scale (arcsec)	• 0.66 (MAGRITTE) • 0.60 (SPECTRE)
Camera - Focal Plane Array	4096 x 4096, 12 μm, 13 bit/pix
Bandpass (Å)	• MAGRITTE - Fe XII 195 Å - Fe XV 284 Å - He II 304 Å - Fe XVI 335 Å - Ne VII 465 Å - Ly-α 1216 Å • SPECTRE OV 629 Å • GT WL Continuum 6700 Å (500 Å FWHM)
Exposure Times	<8 sec
Synoptic Cadence	• AIA 10 sec • GT 50 Hz
Maximum Cadence (sec)	2.5 sec full disk, full resolution
Aperture (mm)	• 45 mm (EUV), 60 mm (Ly-α) (MAGRITTE) • 80 mm (OV) (SPECTRE) • 39 mm GT
Effective Focal Lengths	• 3.75 (MAGRITTE) • 4.00 SPECTRE • 1.30 GT
Required absolute pointing	1 arcmin
Required pointing stability	<1.2″ during exposures (8 sec). Requires GT/IMC
Mechanism Count	7 shutters, 7 aperture doors, 6 filter covers, 7 IMC

3. MAGRITTE : FILTERGRAPH TELESCOPES – NARROWBAND MULTILAYERS

3.1 MAGRITTE concept

An off-axis optical design was chosen as compromise between the optical performances, the large field of view and the baffling characteristics. The telescopes will image a 45 arcmin FOV with an effective focal length of 3.75 m. The optical layout is detailed in figure 2.

The Ly-α channel is based on the rocket-borne Transition Region Camera[5] design which uses narrow-band interference filters to isolate Ly-α. It has been adapted for compactness by using a scheme nearly identical to the multilayer instruments: an off-axis Ritchey-Chretien design with a 60 mm (resized for throughput and diffraction) aperture.

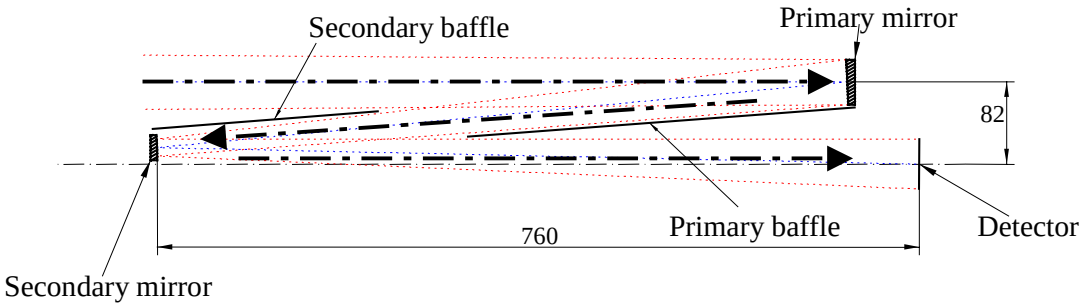

Figure 2: Optical layout of Filtergraph off-axis Ritchey-Chretien telescopes (in mm). Due to the diffraction limit and throughput, the Ly-α channel will be slightly larger

The wavelengths for the filtergraph telescopes were selected according to science criteria and technical considerations and all are based on a common conceptual design, illustrated in figures 3, 4 & 5.

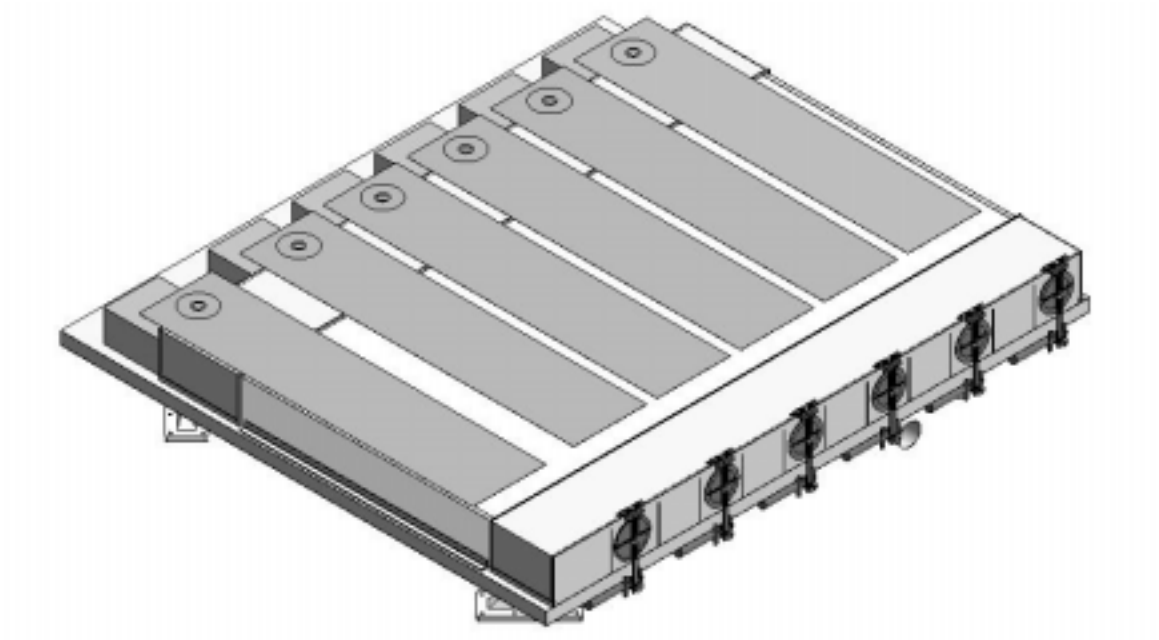

Figure 3: MAGRITTE instrument

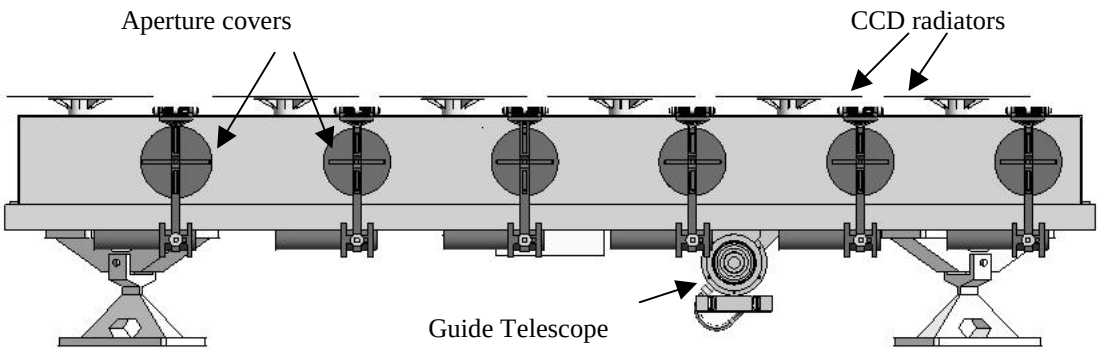

Figure 4: Front view of MAGRITTE

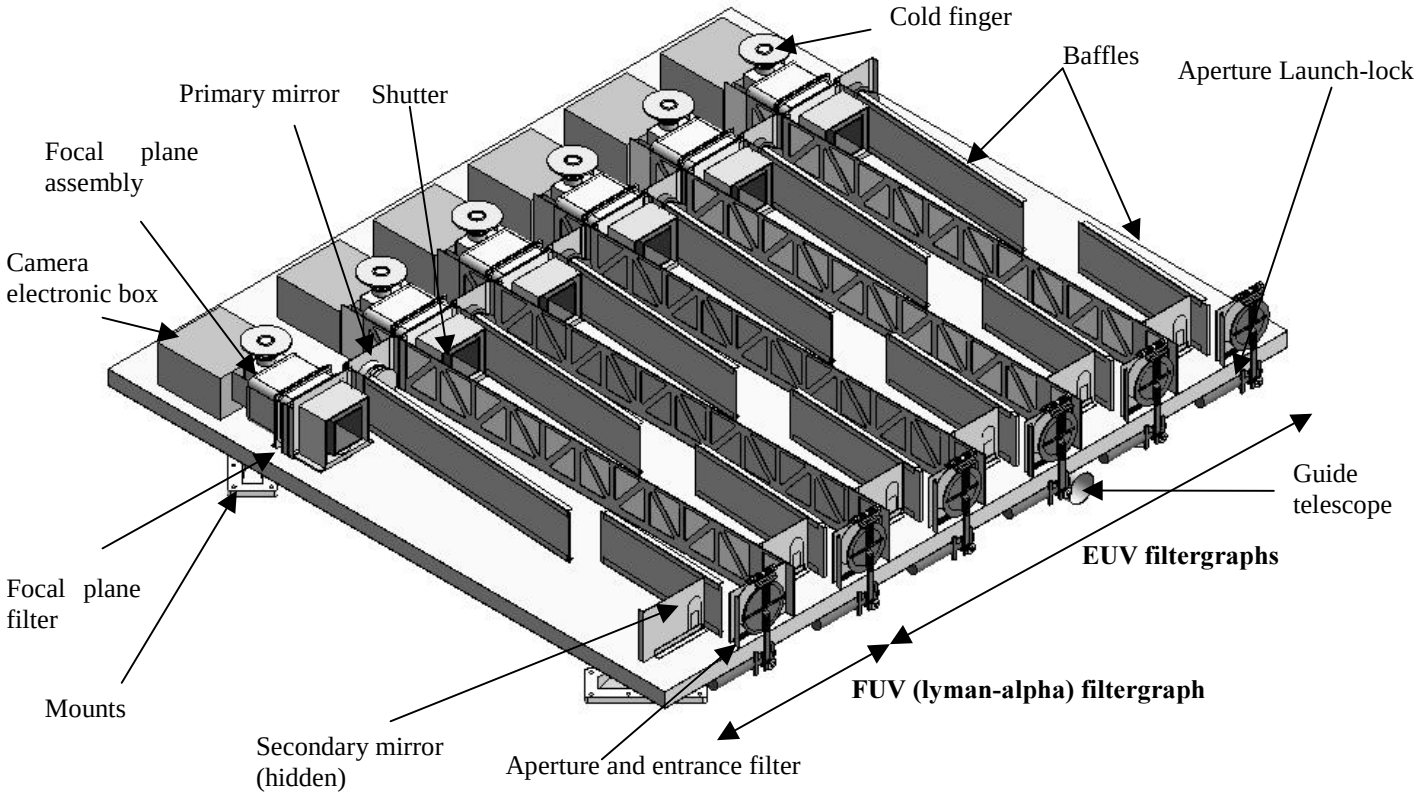

Figure 5: Open view of the MAGRITTE instrument

3.2 MAGRITTE Optics

The optics for all the filtergraph channels will be developed by IOTA. The optical prescription is detailed in table 3. After reaching a spherical shape, the off-axis figuring will be obtained with ionic beam polishing at the IOTA facility. Multilayer EUV coatings will be optimized for the off-axis system, with non-normal incident angles. The 195, 284 and 304 Å channels will be similar to the STEREO/EUVI[6] coatings (also heritage and significant improvements from SOHO-EIT[4]).

New developments will be conducted to define, prepare, optimize and test coatings for 335 and 465 Å. For Fe XVI (335 Å), standard materials (Si, Mo) or recently tested materials (B_4C, Si; baseline) will be used, while there remains several possibilities for the Ne VII (465 Å) line. One is the use of a multilayer originally devised by Seely (NRL) consisting of scandium-silicon with a thin tungsten barrier layer to prevent interdiffusion at the Sc-Si interfaces and improve stability of the multilayers (Sc-W-Si-W multilayer). This multilayer has been successfully applied on a replica of the Skylab grating in order to obtain laboratory measurements of the optical constants for Scandium. These new optical constants, plus the stabilizing tungsten barrier, form the basis for our reflectivity calculations for this channel.
The other alternative for the 465 Å channel uses new materials such as Ti and B_4C.

The Ly-α channel has multilayer coatings on the primary and secondary of $Al/MgF_2/B_4C$[10] optimized for reflectivity at 1215 Å. The filtergraph system is fully baffled with two internal, planar baffles. The compact, off-axis design provides high throughput with straightforward baffles and no obstruction by a mirror support spider.
The design has been optimized for easy to achieve baffle tolerances while simultaneously avoiding any vignetting in the FOV.

Table 3: Optics Definition MAGRITTE Telescopes

Element	Curvature (mm)	Conic	Distance (mm)	Remark
Primary Mirror				Circular
EUV	1730.5	-1.01	690	45mm dia. EUV , off-axis 82 mm
Ly-α	1730.5	-1.02	690	60mm dia. Ly-α , off-axis 100 mm
Secondary Mirror				Circular (25mm)
EUV	455.5	-2.75	760	Off-axis: 16.5mm
Ly-α	455.5	-2.70	760	Off-axis: 20.3mm
Detector	Flat	N/A	N/A	Plate Scale: 0.66 arcsec/pixel EUV tilted around θ_x by -0.62° Ly-α tilted around θx by –0.5°

3.3 MAGRITTE Filters

The EUV light enters the instrument through an aluminum filter that suppresses most of the UV, visible and IR counterparts of the solar radiation. Custom Luxel filters with 1500 Å thick aluminum layer supported by a nickel grid are considered for the baseline. The grid will provide mechanical strength and adequate conductive path for heat excess. Alternate solutions will be vigorously investigated in Phase A to either reduce the diffraction effects or improve the mechanical strength. Wider mesh grids or composite filters (stack of Al layers with spacer material such as boron or silicon) may offer superior solutions. Alternative locations for the second filter will be considered, taking into account diffraction and shading effects that the opaque supporting grid may produce.

Two narrow-band interference filters will be used to achieve the spectral purity for the Ly-α channel. One filter will be placed at the entrance aperture (where it will reject X-rays and protect the secondary mirror coating with a visible light rejection of 10^{-4}). The second filter will be placed in front of the focal plane and will provide adequate redundancy. The combination of these filters yields a spectral purity of 87% for Ly-α in the quiet sun and higher purity in active regions. It is instructive to contrast this instrument with the Ly-α channel on TRACE that was also based on the TRC design. In order to observe both 1550 Å C IV and Ly-α with a single mirror, TRACE used a coating optimized for C IV combined with a Ly-α filter, resulting in a double-peaked response[11]. The TRACE filtergrams therefore consist of only ~50% Ly-α with the bulk of the residual a mixture of continuum and C IV. Our design, fully optimized for Ly-α, will produce significantly spectrally purer images, similar to the original Bonnet TRC.

3.4 CCD

All the CCDs are individually connected to their respective cold fingers and radiators, which will allow independent thermal control.
The detectors are identical thinned, back-illuminated CCDs with 4096 x 4096 pixels of 12 microns pitch. The CCDs will be passively cooled down to -100°C with radiator facing cold space. This will minimize the dark current and provide a better resistance to radiations.
All the detectors will be closely linked to a heater in order to bake-out periodically the contaminant layer that could build up on the cold surfaces of the sensors.
Additional shielding against important radiation levels seen in a the SDO GEO orbit will be implemented and will be part of the housing of the FPA.

3.5 MAGRITTE mechanisms

The six telescopes use identical mechanisms:

1. A one-shot aperture door mechanism: the initial design of the mechanism is based on the INTEGRAL/OMC (launched and successfully operated in space in Oct-2002) and COROT (under development) aperture systems. It uses a spring-loaded hinge with plain bearings, and a paraffin actuated launch lock device (Starsys RL-50C) that was implemented in the SOHO/EIT and INTEGRAL/OMC aperture mechanisms
2. One shutter per telescope used for selecting exposure time (cadence ~10s) and allowing detector lecture. It is developed at MPAe.

3. Possible retractable protection of the thin entrance aluminum filter to avoid breaking of the filter during launch (internal door).
4. Image motion compensation system (IMC) on the secondary mirror (piezo-based system, tilts along 2 axes, small amplitude, no locking mechanism).

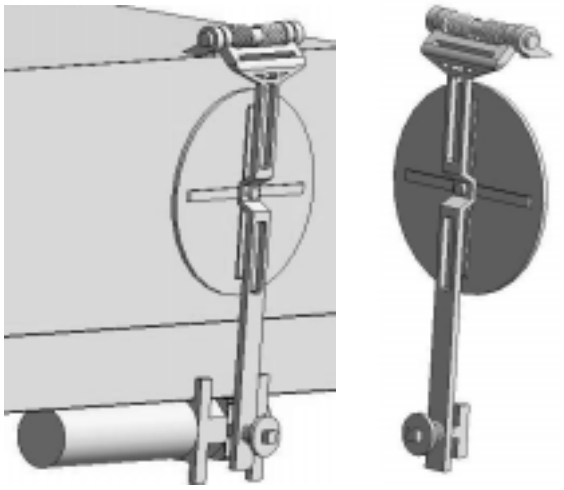

Figure 6: Conceptual view of the door mechanisms

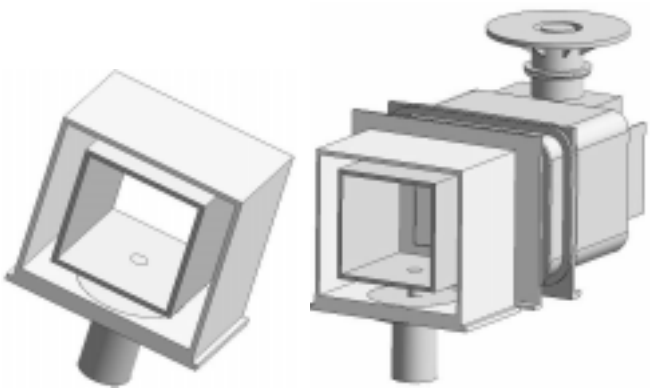

Figure 7: Conceptual view of the shutter mechanism (alone, left) with the focal plane assembly (right)

3.6 Optical bench and housing

The optical performances are highly sensitive to variations of the distance primary – secondary mirrors. In order to keep an acceptable thermal degradation, the inter-mirror distance variation is limited to ± 30 µm from its nominal (ground alignment) value. This corresponds to increases of 0.25 arcsec (EUV channels) and 0.45 arcsec (Lyman-α channel), as accounted in the budgets of table 5. These constrains dictate one of the main requirements on the thermal design of MAGRITTE in order to define the optical bench material and thermal control.
The internal elements of each unit are mounted on a common optical bench that provides the required thermo-mechanical stability. A CFRP (M55J carbon fibers) optical bench will keep the optics immune from the thermo-mechanical variations. CFRP panels for baffling and envelope purposes will encase each unit. Dismountable panels will allow easy access to internal elements from the front (instrument entrance: aluminum filters, filter protection, secondary mirrors) and the rear sides (focal plane assemblies, primary mirrors, shutters).
The off-axis optical design has been optimized for large baffle tolerances while simultaneously avoiding any vignetting in the FOV. In consequence, the optical baffles will not require alignment adjustments.

The overall structure will be connected to the spacecraft with a set of isostatic mounts that will reduce stresses and deformations on the optical bench in all the flight conditions., as well as the conductive thermal flux from the spaceraft platform. One of these mounts is illustrated in figure 8.

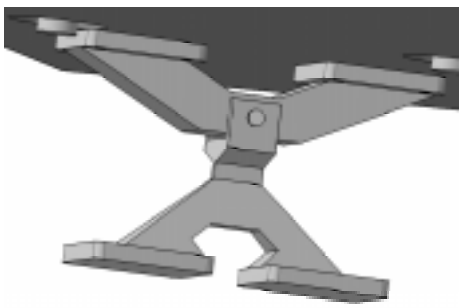

Figure 8: Preliminary design of the isostatic mounts

3.7 Thermal design

The thermal design of the instrument is studied

- to keep a stable average temperature on the optical bench (minimum variation between BOL and EOL, eclipses periods);
- to limit the gradient and avoid bending of the optical bench (to avoid mirrors misalignment);
- to maintain all the subsystems (mechanisms, glue, ...) within acceptable temperature ranges;
- to be able to compensate for input power loss resulting from a CEB failure;
- and to maintain the optics at a warmer temperature than the surroundings (to avoid molecular contamination).

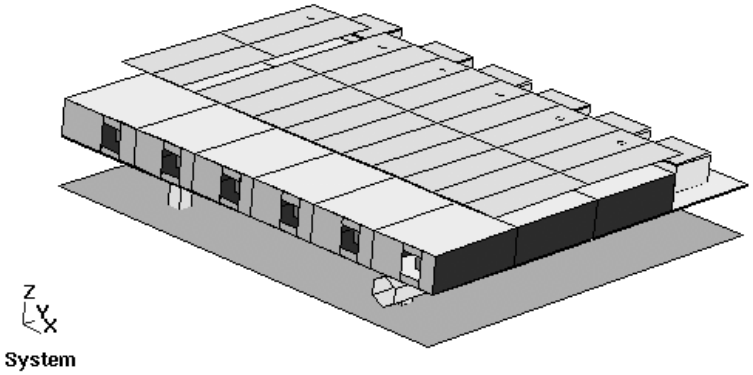

Figure 9: MAGRITTE thermal model

A thermal model has been built to study the thermal behavior of the instrument. It includes the Sun input on the front section, the power dissipation for each CEB box and the power dissipation at the FPA level for CCD heat input. The external environment is modeled with reduced heat sink temperatures. The cold case corresponds to the beginning of life conditions (thermal coating efficiencies) , with a 1250 W/m² constant solar flux (seasonal variation, cold case), while the hot case represents the end of life conditions, with a 1415 W/m² solar flux. The preliminary results of the thermal analysis are summarized with the temperature maps of the internal parts of MAGRITTE, shown in figure 8, with the warmest internal element being the entrance filter, and the coldest the cold fingers.

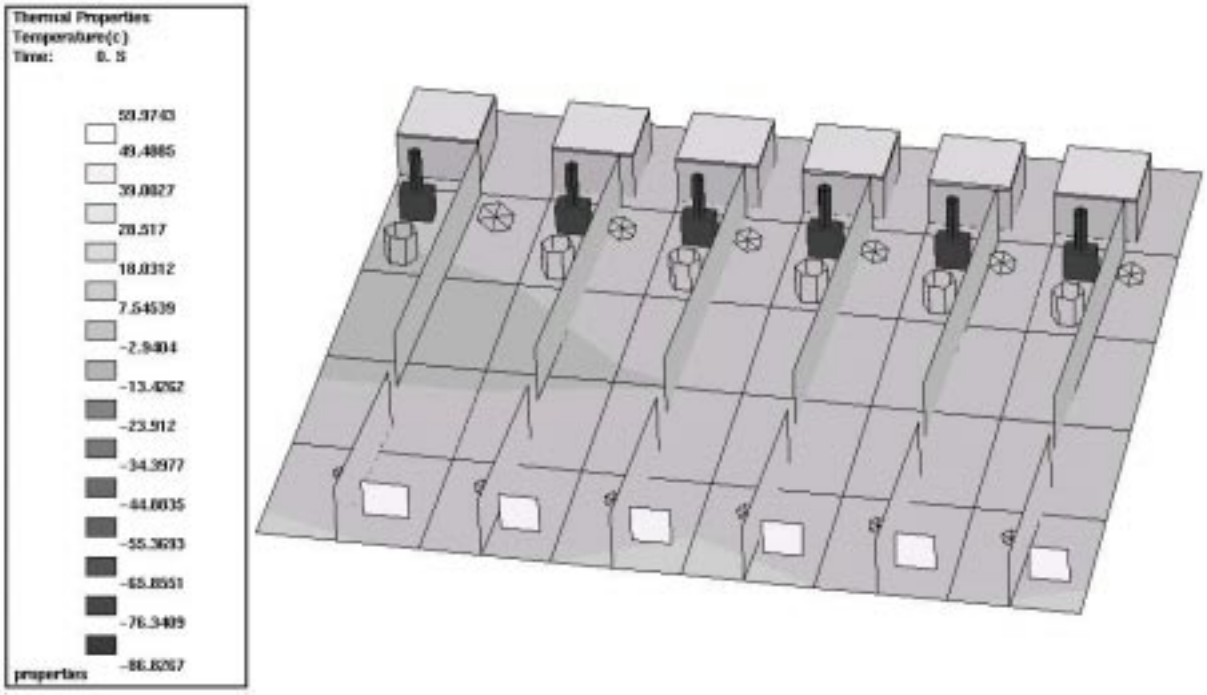

Figure 10: Temperature map of the internal parts of MAGRITTE in one thermal configuration

3.8 MAGRITTE Instrument Performance

– ***EUV optical performances***

The figure 11 shows the optical performances of MAGRITTE, by characterizing the diameter that encircles 70 % of the spot energy. The optical design is diffraction limited over 32 arcmin FOV (from –16 to +16 arcmin) and design limited outside. The best focus is set at 12 arcmin. The design produces a spot inside the pixel (0.66 arcsec) over a circular 45 arcmin FOV. The table 4 summarizes the range where the design is diffraction limited for each EUV channel.

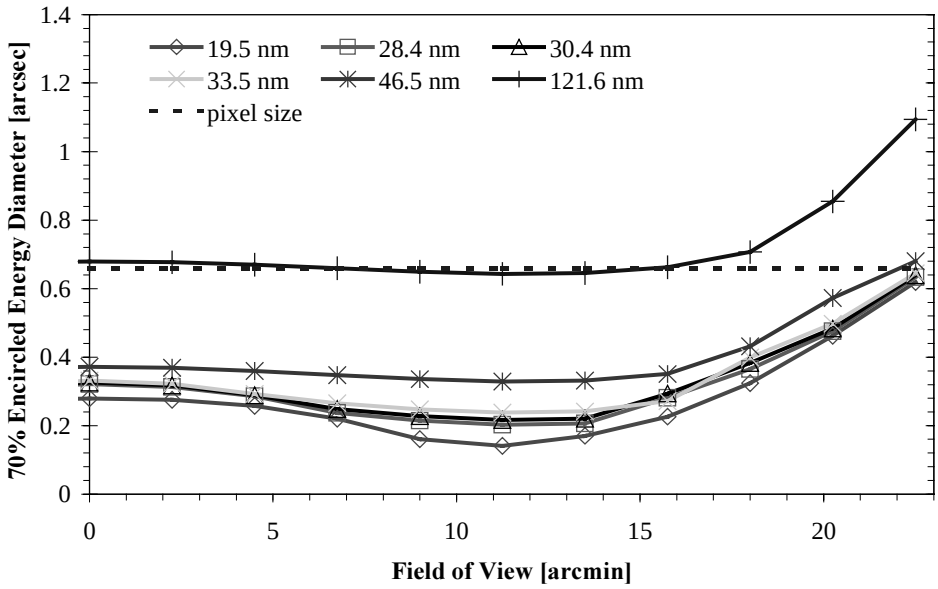

Figure 11: Optical performance of Magritte, 70% encircled energy diameter

Wavelength	Theoretical Airy diameter	Diffraction limited range
195 Å	0.218 arcsec	-16.5 to -4 arcmin 4 to 16.5 arcmin
284 Å	0.317 arcsec	-18 to 18 arcmin
304 Å	0.339 arcsec	-18.5 to 18.5 arcmin
335 Å	0.374 arcsec	-19 to 19 arcmin
465 Å	0.52 arcsec	-21 to 21 arcmin

Table 4 : Theoretical Airy disk and FOV range where the design is diffraction limited

The table 5 summarizes all degradation contributions. Including tolerances, the 70% encircled energy geometric is included into a 4 pixels area (1.32 x 1.32 arcsec²). The main contribution comes from the wavefront error of mirrors. This contribution depends largely on the kind of figuring error on both mirrors. Therefore polishing and measurement have very stringent requirements. The total of the contributions of table 5 is based on an rms sum for all the terms except the design contribution that is arithmetically added.

– ***FUV optical performances (Lyman-α channel)***

The figure 11 shows the optical performances of the nominal design in terms of the 70% encircled energy diameter. The optical design is diffraction limited over the 45-arcmin circular FOV. In the corner of the CCD, the spot is larger.
The degradation contributions are also detailed in table 5. Including tolerances, the 70% encircled energy geometric is included into a 4 pixels area (1.32 x 1.32 arcsec²). Similarly to the EUV telescopes, the main contribution comes from the WFE of mirrors. So polishing and measurement will also need to be accurate.

Table 5: Optical performance contributions in terms of 70% encircled energy geometric degradation (ΔΦ)

Contributions	EUV channels		FUV channel (Ly-α)	
FOV	**On-axis**	**12 arcmin FOV**	**On-axis**	**At 12 arcmin FOV**
Design	0.26 arcsec	0.08 arcsec	0.31 arcsec	0.13 arcsec
Mirrors manufacturing	0.07 arcsec	0.07 arcsec	0.126 arcsec	0.126 arcsec
Alignment	0.08 arcsec	0.08 arcsec	0.055 arcsec	0.055 arcsec
Mirror WFE	0.62 arcsec	0.769 arcsec	0.44 arcsec	0.605 arcsec
Thermo-optical degradation	0.47 arcsec	0.47 arcsec	0.45 arcsec	0.45 arcsec
Total	**1.045 arcsec**	**0.903 arcsec**	**0.954 arcsec**	**0.896 arcsec**

4. MAGRITTE RESPONSES AND EFFECTIVE AREAS.

The efficiency of all the elements of MAGRITTE has been measured in previous programs or extrapolated from component measurements. The 195, 284 and 304 Å multilayers reflectivities are based on recent measurements (CALROC/EIT, SECCHI/EUVI mirrors); the 335 and 465 Å values are theoretical estimates based on measured optical constants. The 335 Å coating will use B_4C/Si layers, while the 465 Å will require Sc/Si layers, for which we have used the measurements recently performed by NRL. Peak reflectivity for the EUV mirrors range from 15-40% depending upon the particular band.

The aluminum filter data are using Luxel filter properties for 1500 Å aluminum layer, including the grid transmission (82%) and an oxide layer. The CCD quantum efficiencies were derived from the Marconi (E2V) CCD42 performance and range from 80-90% for the EUV lines, 25% at 1215 Å. Those data were convolved with the Solar input spectrum from the Chianti database[7], to derive the overall instrument response, as detailed in table 6. This table shows the predicted signal-to-noise (photon statistics) achieved in an 8 second exposure and indicates that the MAGRITTE design is compatible with a 10 s cadence (8 second exposure plus 2 second CCD readout) for all the channels. The exact exposure time will be optimized for each channel with the goal of having active regions intensities no more than 1/3 full well, in order to allow for flare detection. The effective area is defined as the product of the optical efficiencies (geometric area, mirror reflectivity, filter transmission, and quantum efficiency) and is shown in figure 12 for the 6 channels of MAGRITTE.

Table 6:MAGRITTE Channels with photon statistics

Channel Å	Temperature Response	Quiet Sun S/N	Active Region S/N
195	1.5 MK	20	100
284	2.0 MK	N/A	50
304	80,000 K	30	114
355	3.0 MK	N/A	41
465	0.7 MK	8	26
1216	20,000 K	34	100

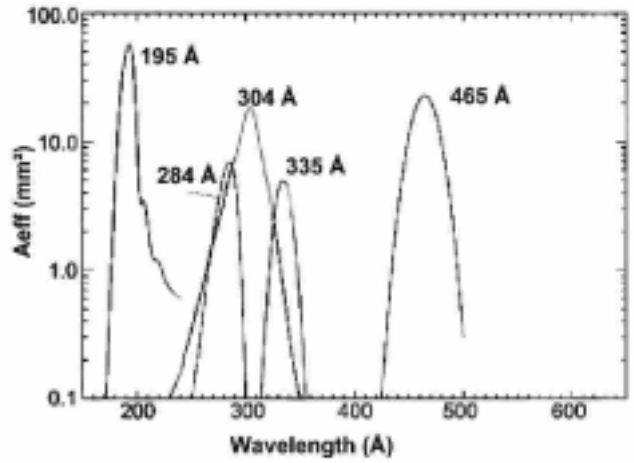

Figure 12: MAGRITTE EUV channels instrument efficiencies

5. CONCLUSION

A new set of EUV instruments is being prepared for the SDO mission. They will provide simultaneous high angular and temporal images in 6 EUV channels and one FUV channel. The phase B of the project will start in the second half of 2003. New assessment studies and breadboarding activities will confirm the design options.

6. ACKNOWLEDGMENTS

The MAGRITTE instruments are developed by Centre Spatial de Liège (Belgium), the Institut d'Optique Théorique et Appliquée (IOTA, Orsay, F), the Max Planck Institut für Aeronomie (MPAe Lindau, G) and the Naval Research Laboratory (NRL, USA).
The Belgian contribution to the SHARPP program is funded by the Federal Office for Scientific, Technical and Cultural Affairs (OSTC), in the frame of the ESA/Prodex program.

7. REFERENCES

1. P. Rochus, J.M. Defise, J.P. Halain, E. Mazy, R.A. Howard, J.D. Moses, J. Newmark, F. Clette, P. Cugnon, D. Berghmans, J.F. Hochedez, J.P. Delaboudinière, G. Artzner, F. Auchère, R. Mercier, M.F. Ravet, F. Delmotte, M. Idir, E. Antonucci, S. Fineschi, D. Gardiol, M. Romoli, M. Malvezzi, P. Nicolesi, G. Naletto, R.A. Harrison, U. Schühle; "MAGRITTE / SPECTRE : the Solar Atmospheric Imaging Assembly (AIA) aboard the Solar Dynamics Observatory", AGU Fall Meeting, Dec-2002.
2. S. Fineschi et al., "SPECTRE: the spectroheliograph for the transition region aboard the Solar Dynamics Observatory", SPIE **5171** (this volume), 2003.
3. J.D. Moses; "Solar & Heliospheric Activity and Prediction Program (SHARPP) for SDO" , SPIE **5171** (this volume), 2003.
4. JP. Delaboudinière, G.E. Artzner, J. Brunaud, A.H. Gabriel, J.F. Hochedez, F. Millier, X.Y. Song, B. Au, K.P. Dere, R.A. Howard, R. Kreplin, D. J. Michels, J.D. Moses, J.M. Defise, C. Jamar, P. Rochus, J.P. Chauvineau, J.P. Marioge, R.C. Catura, J.R. Lemen, L. Shing, R.A. Stern, J.B. Gurman, W.M. Neupert, A. Maucherat, F. Clette, P. Cugnon, E.L. Van Dessel., "EIT: Extreme-UV imaging telescope for the SOHO mission"; Solar Physics **162:** 291-312, 1995.
5. R.M. Bonnet, E.C. Bruner, L.W. Acton, W.A. Brown, M. Decaudin, "High resolution Lyman-alpha filtergrams of the Sun", Astrophysical Journal **237**:L47-L50, 1980.
6. R. A Howard, J.D. Moses, D. G. Socker and the SECCHI consortium, "Sun Earth connection coronal and heliospheric investigation"; *SPIE* **4139**, 2000.
7. K.P. Dere, E. Landi, H.E. Lanson, B.C. Monsignori Fossi, P.R. Young, "CHIANTI", A&A Supp., **125**, 149, 1997.
8. Prinz, D. 1973, Sol. Phys., 28, 35
9. Moses, J. D., et al. 1997, Sol. Phys., 175, 571
10. Juan I. Larruquert, Ritva A. M. Keski-Kuha, Applied Optics-OT, Vol. 38 Issue 7 Page 1231 (March 1999)
11. Handy, B. et al. 1999, Sol. Phys., 190, 351